

# Intracavity phase conjugation of the radiation from a pulsed frequency-selective CO laser

A A Ionin, A A Kotkov, A K Kurnosov,  
A P Napartovich, L V Seleznev

**Abstract.** The temporal dynamics and efficiency of phase-conjugate reflection in the course of intracavity degenerate four-wave mixing of radiation from a pulsed frequency-selective electron-beam-sustained CO laser was investigated experimentally and theoretically. The energy efficiency of the phase-conjugate reflection in the experiments reached 1.5–2.5% for a CO laser emitting as a result of one vibrorotational transition, diminishing on expansion of the emission spectrum of the laser. Comparison of the experimental and calculated data indicates the dominant role of the resonance amplitude phase-conjugation mechanism in the active medium of a CO laser.

## 1. Introduction

Degenerate four-wave mixing (DFWM) in the active medium of the laser itself is apparently (as for high-power CO<sub>2</sub> lasers [1–4]) the most promising method for the phase conjugation of the radiation from high-power carbon monoxide lasers. A signal with a scattering coefficient up to 0.1 was observed [5, 6] in the loop system for the DFWM of the radiation from a pulsed nonselective gas-flow electron-beam-sustained (EBS) laser when this radiation was backscattered in the active medium of a laser amplifier. When an intracavity DFWM system was used in the active medium of a multifrequency pulsed EBS CO laser [7], the efficiency of the phase-conjugate reflection was ~0.2%.

The theory of DFWM processes in the radiation from a multifrequency CO laser in the active medium of the amplifier was developed in Refs [6, 8, 9], where it was shown that the multifrequency character of the CO-laser radiation leads to the appearance in the active medium of a set of amplitude gratings of the gain, the diffraction properties of which depend in a complex manner on the phase relations between them. The emission of the CO-laser radiation as a result of a large number (10–30) of vibrorotational transitions considerably complicates the analysis of the phase-conjugation process because in the active medium of this laser each gain grating is formed not only under the influence of the

radiation emitted because of the transition in question, but also (as a consequence of the cascade lasing mechanism) under the influence of the radiation resulting from neighbouring vibrational transitions.

The use of a frequency-selective CO laser emitting as a result of selected vibrorotational transitions makes it possible to simplify the comparison of experimental data with the results of calculations and to estimate the mutual influence of the emission of radiation in various vibrational bands under the DFWM conditions.

This communication presents the results of an experimental and theoretical study of phase conjugation in the intracavity DFWM of the radiation from a pulsed frequency-selective EBS CO laser in its active medium. The energy and time characteristics of the phase-conjugate reflection process are compared with the results of theoretical calculations carried out on the basis of a kinetic model of the active medium of a CO laser [10].

## 2. Experimental set up and experimental methods

The experiments were performed on a pulsed electron-beam sustained laser system with cryogenic cooling of the CO–N<sub>2</sub>–He active gas mixture to ~120 K. The optical system in the experiments on the intracavity radiation from a frequency-selective EBS CO laser in its active medium is presented in Fig. 1. The active medium of laser (1) 1.2 m long was placed at a distance of ~6 m from the output mirror (2). The laser cavity length was 17.7 m. The output windows of the electron-beam-sustained discharge chamber made of CaF<sub>2</sub>, were inclined at the Brewster angle relative to the optical axis of the laser cavity. A plane interference

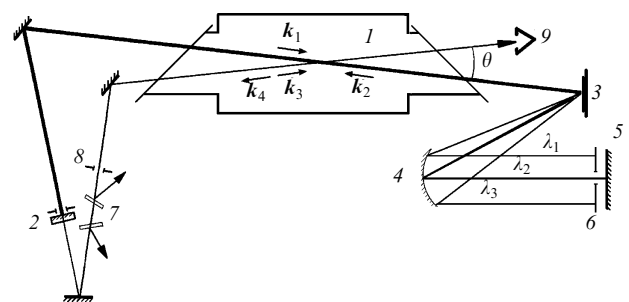


**Figure 1.** Optical setup for intracavity DFWM in the active medium of a frequency-selective EBS laser: (1) active medium of the laser; (2) output mirror of the laser cavity; (3) diffraction grating; (4) spherical mirror; (5) plane mirror; (6) slit optical mask; (7) beam splitters (attenuators); (8) beam-limiting stop; (9) absorber.

A A Ionin, A A Kotkov, L V Seleznev P N Lebedev Physics Institute,  
Russian Academy of Sciences, Leninskii prospekt 53, 117924 Moscow,  
Russia

A K Kurnosov, A P Napartovich Troitsk Institute of Innovative and Fusion  
Research (State Scientific Centre of the Russian Federation),  
142092 Troitsk, Moscow province, Russia

Received 4 October 1999

Kvantovaya Elektronika 30 (4) 342–348 (2000)

Translated by A K Grzybowski

mirror with a reflection coefficient of  $\sim 40\%$  in the wavelength range  $5.2\text{--}5.6\ \mu\text{m}$  was used as the output mirror (2) of the cavity. The aperture of the output laser beam ( $\sim 15\ \text{mm}$  in diameter) was limited by an intracavity stop in front of the output mirror. The duration of an EBS CO laser radiation pulse amounted to hundreds of microseconds for a duration of the electron-beam-sustained discharge pulse of  $\sim 30\ \mu\text{s}$ . The emission spectrum of the laser radiation in the case of a nonselective cavity of a CO laser consisted of a large number of lines (10–30), the most intense of which were in the wavelength range  $5.2\text{--}5.6\ \mu\text{m}$  and corresponded to vibrational transitions from  $8 \rightarrow 7$  to  $12 \rightarrow 11$  with an energy maximum on the rotational transitions  $J - 1 \rightarrow J$  with  $J = 13\text{--}15$ . The small-signal gain in the active medium of the laser reached  $1.8\ \text{m}^{-1}$  for an energy input of  $\sim 400\ \text{J litre}^{-1}\ \text{amagat}^{-1}$ .

An intracavity diffraction grating (3) (blaze angle  $\sim 30^\circ$ ,  $100\ \text{grooves mm}^{-1}$ ) was used for the selective regime in the operation of the CO laser. The grating, operating in the Littrow scheme in the second diffraction order, was used, first, as the spectral selector (the polarisation plane and the plane of the incidence of radiation on the grating surface were almost perpendicular to the direction of grating lines) and, second, as a deflecting mirror in the plane parallel to the gratings grooves. The grating (3) was placed in the focal plane of a spherical mirror (4) with a radius of curvature of  $\sim 3\ \text{m}$ .

The spherical mirror directed the laser beam to a plane rear mirror (5) placed beyond the focal plane. The position of this mirror relative to the focal plane determined the effective radius of curvature ( $\sim 40\ \text{m}$ ) of the equivalent selective mirror [11], consisting of the diffraction grating (3), the spherical mirror (4), and the plane mirror (5). A slit optical mask (6), located ahead of the plane mirror (3), was used to select the spectral lines corresponding to definite vibrotational transitions of the CO molecule. The spectral composition of the laser radiation as specified by the configuration of the optical mask (6), i.e. by the number, width, and positions of the slits.

A probe wave  $k_3$  intersected the reference waves  $k_1$  and  $k_2$  at the centre of the inverted active medium at the angle  $\theta \approx 10\ \text{mrad}$  relative to the copropagating wave  $k_1$ . For the specified angle of convergence of the laser beam  $\theta$ , the length of the interaction region of the radiation was virtually identical with the length of the active medium of the laser. In order to fulfil the condition of temporal matching between the probe and copropagating reference waves, the optical delay between them did not exceed  $0.1\ \text{m}$ . The energy (or intensity) reflection coefficient of the phase-conjugation mirror was measured by comparing the energies (intensities) of the phase-conjugation and probe signals.

The channel for the measurement of the energy of the phase-conjugation signal was calibrated by using the probe signal backreflected either by a plane metal mirror (employing calibrated attenuators) or by one face of an optical  $\text{CaF}_2$  wedge. In these calibrations, the backreflecting surface was located directly beyond the beam-limiting stop  $11\ \text{mm}$  in diameter placed in the path of the propagation of the probe wave in order to reduce the background radiation from the laser cavity. Experimental data, which make it possible to judge the phase-conjugation quality in the course of the intracavity DFWM and indicate that the backreflected signal is indeed a phase-conjugation signal, were published previously [7].

A system of recording the parameters of the laser radiation made it possible to measure the energy of the probe and phase-conjugation signals and their temporal dynamics, to determine the distribution of radiation in the near and far-field zones, and to record the emission spectrum. The energy of the radiation pulses was measured with thermocouple calorimeters. The temporal profile of the radiation pulses was recorded by a Ge: Au photodetector with a time resolution of  $\sim 10^{-6}\ \text{s}$ . The emission spectrum of the CO laser was recorded by a CO Laser Spectrum Analyser (Model 16-C). The IR radiation was visualised by a thermovision system.

### 3. Energy characteristics of phase conjugation by four-wave mixing

The influence of the specific input energy, the density of the gas mixture, and the ratio of the intensities of the reference and probe waves on the energy efficiency of the phase conjugation was investigated experimentally for various spectral compositions of the laser radiation. The following standard experimental conditions were chosen: composition of the active mixture of gases  $\text{CO}:\text{N}_2:\text{He} = 1:4:5$ , gas-mixture density  $0.3\ \text{amagat}$ , gas-mixture temperature  $120\ \text{K}$ .

The dependences of the efficiency of phase conjugation in the course of four-wave mixing on the parameters of the active medium and the optical cavity was investigated for a selective CO laser operating as a result of one of the three vibrational transitions of the CO molecule. The radiation wavelengths at the centre of each spectral range were chosen to be  $5.23\ \mu\text{m}$  (vibrational transition  $8 \rightarrow 7$ ),  $5.39\ \mu\text{m}$  (transition  $10 \rightarrow 9$ ), and  $5.52\ \mu\text{m}$  (transition  $12 \rightarrow 11$ ). The spectral width of each range was specified by the slit width in the optical mask (6) and amounted to  $\sim 15\ \text{cm}^{-1}$ . The laser emission spectrum consisted of lines corresponding to several rotational transitions of the CO molecule (from one–two in the region of  $5.23$  and  $5.52\ \mu\text{m}$  to three–four in the region of  $5.39\ \mu\text{m}$ ). When the input energy was reduced, one most intense line was selected in the emission spectrum. For each of the spectral ranges, the radiation pulse energies of the most intense  $5.23$ ,  $5.39$ ,  $5.52\ \mu\text{m}$  lines amounted respectively to  $0.42$ ,  $1.0$ , and  $0.72\ \text{J}$  for a specific input energy of  $\sim 300\ \text{J litre}^{-1}\ \text{amagat}^{-1}$ .

The specific input energy was varied in the experiments from  $100$  to  $400\ \text{J litre}^{-1}\ \text{amagat}^{-1}$ . In contrast to the  $\text{CO}_2$  laser [3], the energy efficiency of the phase-conjugate reflection in the active medium of an EBS CO laser was almost independent of the specific input energy. It is noteworthy that, with increase in the latter from  $100$  to  $400\ \text{J litre}^{-1}\ \text{amagat}^{-1}$ , the laser-radiation pulse energy increased (for example by a factor of  $2.5$  for the vibrational transition  $8 \rightarrow 7$ ) and its duration fell (from  $350$  to  $150\ \mu\text{s}$  for the same transition) as a consequence of the heating of the gas. Thus the intensity of the radiation within the cavity increased, but the energy reflection coefficient of the phase-conjugate mirror remained constant under these conditions.

The change in the ratio of the intensities of the reference ( $I_1$ ) and probe ( $I_3$ ) waves, as the intensity of the probe wave was varied with the aid of calibrated attenuators, exerted a greater influence on the efficiency of the phase-conjugate reflection (Fig. 2). With increase in the ratio  $I_1/I_3$  from  $1$  to  $8$ , the experimental reflection coefficient  $R$  (curve 1) increased by a factor of  $1.5$ . However, on further decrease in the probe-wave intensity (the ratio  $I_1/I_3$  increased to  $18$ ), it changed only slightly. The calculated reflection coefficient (curve 2)

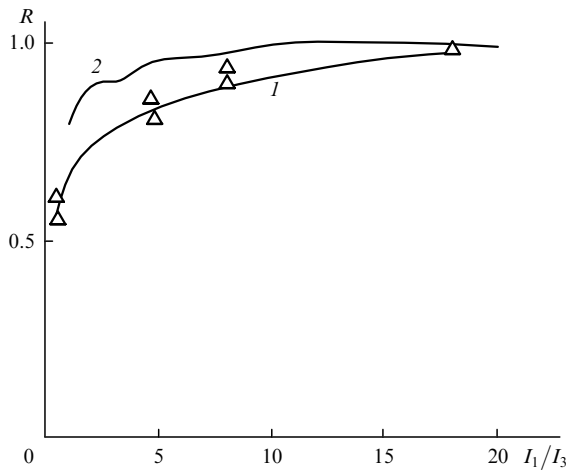


**Figure 2.** Experimental (1) and calculated (2) dependences of the reflection coefficient  $R$  of a phase-conjugate mirror on the intensity ratio  $I_1/I_3$ .

behaves similarly. The same type of dependence of  $R$  on  $I_1/I_3$  was observed also in the case of the active medium of an EBS CO<sub>2</sub> laser [3], where a sharp increase in efficiency was also noted with increase in the ratio  $I_1/I_3$  from 1 to 4, while with increase in  $I_1/I_3$  from 4 to 21 the efficiency of phase conjugation hardly changed.

The influence of the density of the laser mixture on the efficiency of phase conjugation was investigated for the 5.39  $\mu\text{m}$  and 5.23  $\mu\text{m}$  spectral regions with the same Q-factor of the laser cavity. A monotonic increase in the reflection coefficient with increase in the gas density from 0.1 to 0.5 amagat (Fig. 3), similar to its increase in the active medium of an EBS CO<sub>2</sub> laser [3], was observed in the region of 5.39  $\mu\text{m}$ . However, in the region of 5.23  $\mu\text{m}$ , the increase in the reflection coefficient with increase in density occurred only for a gas density less than 0.2–0.3 amagat.

In the study of the influence of the spectral composition of the laser radiation on the energy efficiency of phase conjugation, a combination of three cascade-coupled vibrational transitions with approximately equal radiation-pulse energies was selected:  $P_{8\rightarrow7}(17)$ ,  $P_{9\rightarrow8}(16)$ ,  $P_{10\rightarrow9}(15)$ . In this case, the width of each slit in the optical mask (6) (again Fig. 1) corresponded to the spectral interval between neighbouring

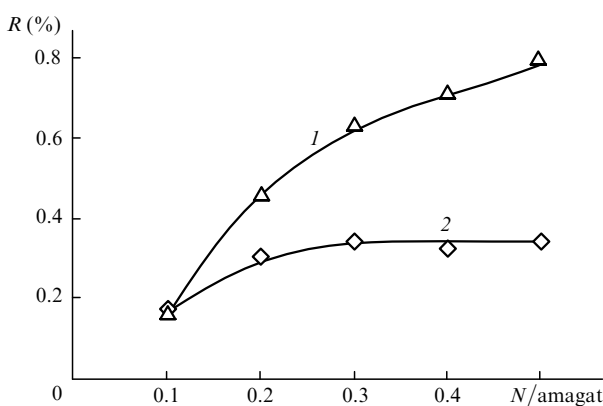


**Figure 3.** Dependence of the reflection coefficient on the density  $N$  of the active mixture for the two spectral regions 5.39  $\mu\text{m}$  (1) and 5.23  $\mu\text{m}$  (2) with a specific input energy of  $\sim 300 \text{ J litre}^{-1} \text{ amagat}^{-1}$ .

**Table 1.** Energy of the laser radiation  $E$  and the phase-conjugation efficiency  $R$  in the operation of a selective EBS CO laser as a result of various combinations of three cascade-coupled vibrational transitions.

| $P_{10\rightarrow9}(15)$ | $P_{9\rightarrow8}(16)$ | $P_{8\rightarrow7}(17)$ | $E/\text{mJ}$ | $R$ (%) |
|--------------------------|-------------------------|-------------------------|---------------|---------|
| +                        | –                       | –                       | 415           | 1.5     |
| –                        | +                       | –                       | 450           | 1.3     |
| –                        | –                       | +                       | 340           | 0.7     |
| +                        | +                       | –                       | 675           | 0.95    |
| +                        | –                       | +                       | 530           | 1.25    |
| –                        | +                       | +                       | 610           | 0.77    |
| +                        | +                       | +                       | 975           | 0.7     |

Note: The specific input energy was  $\sim 300 \text{ J litre}^{-1} \text{ amagat}^{-1}$  and the gas density was 0.3 amagat;  $I_1/I_3 = 8$ . The '+' sign indicates the occurrence of lasing as a result of the relevant transition.

rotational lines of one vibrational band ( $\sim 4 \text{ cm}^{-1}$ ). Table 1 presents the total energies of the laser radiation and the energy efficiencies of phase conjugation for each of the seven combinations of the emission spectrum.

The maximum efficiency of phase conjugation ( $R = 1.5\%$ ) was observed in the emission of laser radiation as a result of one vibrational transition  $P_{10\rightarrow9}(15)$ , while the inclusion of additional cascade-coupled transitions led to a decrease in the efficiency of phase conjugation. The efficiency of phase conjugation with DFWM in a selective cavity for emission with an interrupted cascade (combination of the two lines  $P_{10\rightarrow9}(15)$  and  $P_{8\rightarrow7}(17)$ ,  $R = 1.25\%$ ) was greater than in the case of emission as a result of neighbouring cascade-coupled transitions ( $R = 0.95\%$  for the  $P_{10\rightarrow9}(15)$  and  $P_{9\rightarrow8}(16)$  transitions,  $R = 0.77\%$  for the  $P_{9\rightarrow8}(16)$  and  $P_{8\rightarrow7}(17)$  transitions, and  $R = 0.7\%$  for all three transitions), but smaller than in the case of emission as a result of each individual  $P_{10\rightarrow9}(15)$  and  $P_{8\rightarrow7}(17)$  ( $R = 1.3\%$ ) transition. We may note that, for DFWM in the active medium of a multifrequency (nonselective) EBS CO laser, the efficiency of phase conjugation did not exceed 0.2% [7].

Thus the efficiency of phase conjugation for the intracavity DFWM of the radiation from a frequency-selective CO laser reached a maximum only in those cases where lasing occurred as a result of one vibrational transition for the maximum emission energy. Under the same experimental conditions and with the same selective laser cavity but with a different diffraction grating (blaze angle  $\sim 22^\circ$ , 150 grooves  $\text{mm}^{-1}$ ), operating in the first diffraction order spectrum with a large reflection coefficient in the Littrow scheme, the energy reflection coefficient reached 2.5% for DFWM in the active medium of an EBS CO laser operating as a result of the  $P_{10\rightarrow9}(13)$  transition.

#### 4. Dynamic properties of the phase-conjugate reflection

Fig. 4 presents the time dependences of the envelope [12] of the probe-signal pulse (curve 1) and the intensity reflection coefficient  $R$  (curve 3) for one vibrational transition (5.39  $\mu\text{m}$  spectral region, specific input energy  $300 \text{ J litre}^{-1} \text{ amagat}^{-1}$ ). The maximum intensity reflection coefficient was observed on the leading edge of the laser-radiation pulse (Fig. 4b) and exceeded almost by a factor of two the average reflection coefficient per pulse. Such behaviour of the reflection coefficient was observed on the leading edge of the laser-radiation pulse (Fig. 4b) and exceeded almost by a factor

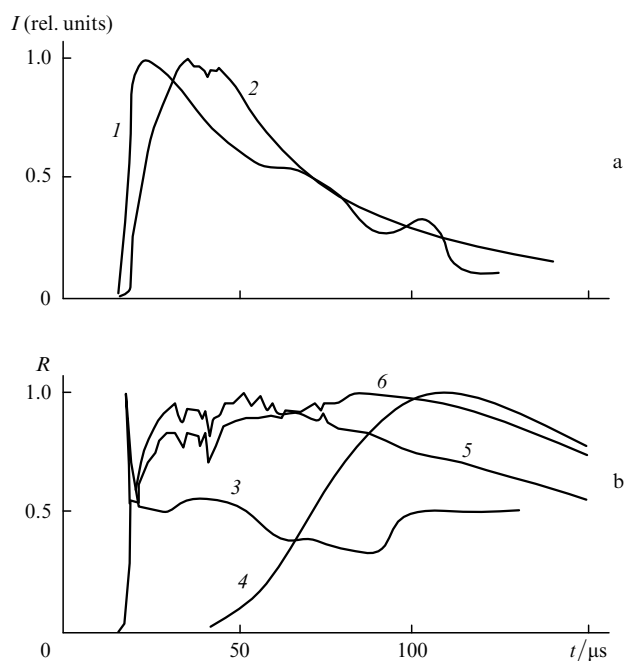


**Figure 4.** Time dependences of the probe signal [experiment (1) and theory (2)]; (a) the intensity reflection coefficient [experiment (3) and the results of the calculation allowing for the refractive index (4) and gain (5) gratings and for both gratings (6)]; (b) in the spectral region of  $5.39 \mu\text{m}$  for a specific input energy of  $\sim 300 \text{ J litre}^{-1} \text{ amagat}^{-1}$ .

of two the average reflection coefficient per pulse. Such behaviour of the reflection coefficient is characteristic of the fast-response resonance mechanism of phase conjugation by four-wave mixing involving amplitude gain gratings. The coefficient  $R$  increased on the leading edge of the radiation pulse because the gain of the active medium exceeded its threshold value [3, 4, 12–14]. For this reason, in calculations based on the quasi-cw lasing model (curve 2), there is no increase in  $R$  (curves 4–6).

In order to compare the temporal behaviour of the reflection coefficient in various parts of the vibrational spectrum of the CO molecule, Fig. 5 presents the probe-wave phase-conjugation signal, and reflection-coefficient pulses for three vibrational bands of the laser radiation for a specific input energy of  $350 \text{ J litre}^{-1} \text{ amagat}^{-1}$ . It is noteworthy that the duration of the laser-radiation pulses increased with increase in the wavelength (from  $\sim 100 \mu\text{s}$  for  $5.23 \mu\text{m}$  to  $\sim 500 \mu\text{s}$  for  $5.52 \mu\text{m}$ ). In all the diagrams (Fig. 5), the temporal dynamics of the reflection coefficient after the first spike of  $1\text{--}2 \mu\text{s}$  duration at the leading edge is characterised by a slow nonmonotonic fall towards the end of the radiation pulse. A similar temporal behaviour of the reflection coefficient was observed also in all the remaining experiments.

Thus, analysis of the temporal dynamics of the phase-conjugate reflection for intracavity DFWM in the active medium of an EBS CO laser indicates that phase-conjugate reflection takes place on the amplitude gratings of the resonance nonlinearity of the active mixture of the laser and has a quasi-cw character with a duration of the transient process of  $1\text{--}2 \mu\text{s}$ . For the theoretical justification of this conclusion, calculations were performed of the reflection efficiency of phase conjugation for the amplitude and phase thermal mechanisms of the nonlinearity based on a kinetic

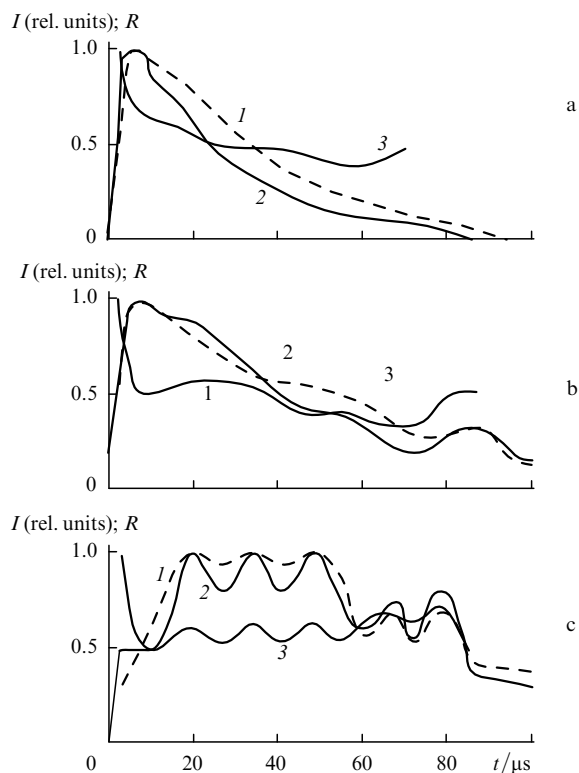


**Figure 5.** Temporal dynamics of the probe (1) and phase-conjugation (2) signal pulses and of the intensity reflection coefficient (3) in the case of lasing as a result of various vibrational transitions in the spectral regions of  $5.23 \mu\text{m}$  (a),  $5.39 \mu\text{m}$  (b), and  $5.52 \mu\text{m}$  (c).

model of the CO laser and the results of these calculations were compared with experimental data.

## 5. Description of the theoretical model

A numerical model, implemented in three stages, was developed for the description of the quasi-cw temporal dynamics of phase conjugation by four-wave mixing in the active medium of a pulsed EBS CO laser. Initially, a calculation was performed for a laser-radiation pulse on a selected transition by using a detailed model of a pulsed CO laser developed earlier [10, 15]. A system of kinetic equations was then solved numerically for the distribution functions of the electrons of the electron-beam-sustained discharge in terms of the energies and populations of the vibrational levels ( $v \leq 52$ ) of CO and  $\text{N}_2$  molecules taking into account the excitation of the molecular vibrations by the electrons of the electron-beam-sustained discharge, the vibrational–vibrational VV-exchange, the VT-relaxation, and the spontaneous and stimulated emission. The threshold gain for each spectral line was calculated from experimental measurements of the radiation losses in the optical components of the laser cavity.

The temporal dynamics of the radiation intensity  $I(t)$  in the active medium of a CO laser, obtained as a result of preceding calculations, was used in the second stage to calculate the dynamics of the gain and the refractive index gratings arising in the active medium for the DFWM of the probe radiation  $I_3$  and the copropagating reference wave  $I_1$  at the angle  $\theta \approx 10^{-2}$  rad. The radiation intensity in the active medium of the laser was specified in the form

$$I(t) = I_1(t) + I_2(t) + I_3(t) + 2(I_1 I_3)^{1/2} \cos(Kz),$$

where  $K = 2\pi\theta/\lambda$  is the wave number of the grating;  $\lambda$  is the wavelength of the emission from the vibrational transition;  $I_1(t) = I_2(t)$  are the intensities of the counterpropagating reference waves in the cavity; all the waves were assumed to be homogeneous in the region where the laser beams overlap.  $M$  equidistant nodes along the transverse  $z$  coordinate ( $M \gg 1$ ) were selected on one half-period of the interference pattern. Local gains on the selected transition and the translational temperatures of the medium were in fact calculated for these nodes by using the full kinetic model of the active medium of an EBS CO laser [10]. The calculation of the temporal dynamics of the amplitude and phase gratings was carried out starting from the instant of the appearance of lasing up to  $t = 200 \mu\text{s}$ .

The temporal dynamics of the amplitude gain gratings differs appreciably from the dynamics of the thermal phase grating in the active medium of an EBS CO laser. The formation of the amplitude grating is determined by gain-saturation processes and its relaxation is determined by the VV-exchange processes between CO molecules, which corresponded to a characteristic time of  $\sim 0.10 \mu\text{s}$  for the radiative transition  $P_{10 \rightarrow 9}$  (13) under the experimental conditions. The gas is heated partly during the VV-exchange and mainly during the VT-relaxation, which is quite fast for  $v \geq 30$ . The rate of heating of the gas during VT-relaxation slows down with increase in the resonance radiation intensity, while the formation of the thermal phase grating in the active medium of the CO laser is comparatively slow. The contribution of the phase grating to the reflection coefficient under the experimental conditions becomes appreciable, according to the calculations, only 40–50  $\mu\text{s}$  after the start of lasing. The amplitude gain grating, tracking the changes in intensity appreciably faster, ensures a dynamic range of the phase conjugation up to characteristic times of  $\sim 10^{-7}$  s.

It has been shown [12, 13] that the radiation pulse from a CO laser has a spiky temporal structure with a spike repetition frequency corresponding to several pulses in the time needed for a round trip in the cavity. If the transverse structure of the radiation is retained from spike to spike, then the model of dynamic gratings in the active medium of an EBS CO laser considered here is applicable to the time-averaged (during the time of the double trip in the cavity) description of the phase-conjugate reflection for intracavity DFWM. An approach formulated earlier [8], based on the solution of coupled-wave equations with DFWM, was used in the third stage to calculate the reflection coefficient. Here, the phase-conjugation signal is the result of the scattering of the intracavity counterpropagating reference wave on the dynamic amplitude and phase gratings.

## 6. Results of numerical calculations and their comparison with experiment

Using the full kinetic model of the active medium of a CO laser, we performed calculations for the dynamics of the amplitude modulation of a spatially homogeneous gain grating  $A_g$  and the power of the light-induced heat evolution  $W_T$ . The results of these numerical calculations showed that the amplitude gain grating  $G$  can be accurately fitted by the expression  $G = G_{\text{th}} + A_g \cos(Kz)$ , where  $G_{\text{th}}$  is the threshold gain and  $A_g < 0$  owing to the saturation of the gain.

Since the time required to establish the thermal grating under the experimental conditions was estimated to be

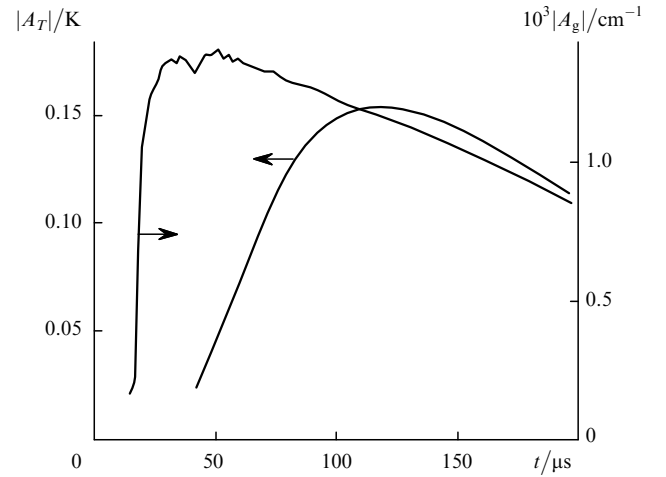


**Figure 6.** Temporal dynamics of the amplitudes of spatial gain and medium-temperature gratings calculated for the conditions in Fig. 4.

$\sim 30 \mu\text{s}$ , the solution of the steady-state thermal conductivity equation may be used to calculate the evolution of the phase grating. The modulation amplitude of the translational gas temperature was estimated from the formula  $A_T = W_T (c_p \chi K^2)^{-1}$ , where  $\chi$  is the thermal diffusivity;  $c_p$  is the heat capacity of the gas at constant pressure. The thermal grating was specified by the expression  $T = T_0(t) + A_T \cos(Kz)$ , where  $T_0(t)$  is the current temperature of the medium averaged over the period of the spatial grating. The resonance radiation in the active medium of a CO laser decreases the rate of heating of the gas during VT relaxation, so that  $A_T < 0$ . Fig. 6 presents the calculated dynamics of the absolute values of  $|A_g|$  and  $|A_T|$  under the conditions of the experiment, the results of which are presented in Fig. 4.

The amplitude (gain) and thermal phase (refractive index) gratings under the experimental conditions proved to be very close to harmonic functions. The analytical solution of the standard equations of coupled waves [16] in the case of harmonic gain and refractive index gratings leads to the expression

$$R = \frac{I_1}{I_3} \left| \frac{\beta \tanh(\gamma d)}{\gamma - \alpha \tanh(\gamma d)} \right|^2, \quad (1)$$

where  $\alpha = G_{\text{th}}/\theta$ ;  $\beta = (0.5A_g - ik\Delta)/\theta$ ;  $\gamma = (\alpha^2 - \beta^2)^{1/2}$ ;  $d = L\theta$  is the transverse dimension of the grating;  $L$  is the length of the interaction region;  $\Delta = A_T/A_0$  is the relative modulation amplitude of the refractive index;  $k = 2\pi/\lambda$  is the wave number. Calculations by formula (1) on the assumption that the gratings are harmonic yield reflection coefficients which agree with those obtained by the numerical method [8], which includes the calculation of the dynamics of the gratings profiles.

Fig. 4a presents the calculated intensity of the quasi-cw laser radiation generated as a result of the  $P_{10 \rightarrow 9}$  (13) transition (curve 2) normalised with respect to the maximum value. Its temporal behaviour is close to the experimental curve 1. Fig. 4b presents the calculated dynamics of the normalised reflection coefficients on the phase grating (curve 4), on the refractive-index grating (curve 5), and when the amplitude and phase gratings are taken into account simultaneously (curve 6). Analysis of the experimental and calculated data showed that the reflection coefficient in the active medium of an EBS CO laser is determined mainly by the amplitude

gain grating. It follows from the analysis of the kinetic model of the DFWM in the active medium of an EBS CO laser that the contributions of the amplitude and phase gratings to the reflection coefficient mutually intensify, so that the resulting effect is appreciably greater than would follow from a simple summation.

On the other hand, if the interference pattern of the field varies with time (for example, as the mode structure of the radiation varies within the cavity), then the slower-responding thermal phase grating proves to be displaced in space relative to the faster-responding amplitude grating. In order to estimate the interaction between the gratings, a numerical experiment was carried out in which the spatial shift of the gratings by 0.2 of a period was specified initially. The calculations showed that, for this kind of shift, the reflection coefficient diminishes appreciably (approximately by a factor of 1.5).

The calculated integral energy efficiency of the phase-conjugate reflection was 9.7% for the amplitude grating and 10.8% for the total effect of the gratings, which exceeds the measured value approximately by a factor of 6. The experimental reflection coefficient is obtained for a twofold decrease in the length of the radiation interaction region  $L$  in expression (1) to  $\sim 0.5$  m. In subsequent calculations, the effective length of the wave interaction region with DFWM was accordingly specified as 0.53 m.

The calculated efficiency of phase conjugation, under the conditions corresponding to Fig. 4, amounted to 1.66% when account was taken only of the amplitude grating and to 1.9% when the amplitude and phase gratings were taken into account simultaneously. The decrease in the effective length of the interaction of the laser beams may be accounted for by the possible instability of the transverse mode structure of the laser cavity and also by the fact that in this experiment (Fig. 4) the emission spectrum consisted of several lines corresponding to the rotational transitions of the CO molecule in one vibrational band. Fig. 2 presents the calculated dependence of the normalised energy reflection coefficient on the parameter  $I_1/I_3$  (curve 2), which demonstrates a quite satisfactory agreement with the experimental curve 1.

The theoretical model was modified in order to analyse the temporal dynamics of the reflection coefficients in the emission of laser radiation simultaneously as a result of several vibrorotational transitions. The calculation was performed initially for the dynamics of lasing as a result of three transitions:  $P_{8\rightarrow 7}(17)$ ,  $P_{9\rightarrow 8}(16)$ , and  $P_{10\rightarrow 9}(15)$  (Fig. 7a). The temporal dynamics of the gain gratings was calculated for the intensity ratio  $I_3/I_1 = 1/8$  and then the intensity reflection coefficient was evaluated (Fig. 7b) on these transitions. The calculation of the energy reflection coefficient on each of the three transitions yielded the following values: 1.28% for the  $P_{10\rightarrow 9}(15)$  transition, 0.91% for the  $P_{9\rightarrow 8}(16)$  transition, and 0.56% for the  $P_{8\rightarrow 7}(17)$  transition.

The efficiency of phase conjugation on the amplitude gratings for three-frequency emission, i.e. when the lasing takes place as a result of all three transitions, was found to be 0.87% in the calculations. It is noteworthy that the calculated ratio of the lasing energies for the above transitions did not agree with the experimental ratio, but the theoretical model describes qualitatively correctly the decrease in the efficiency of phase conjugation as the operating regime of a frequency-selective EBS CO laser changes from lasing as a result of a single vibrorotational transition to the simultaneous lasing as a

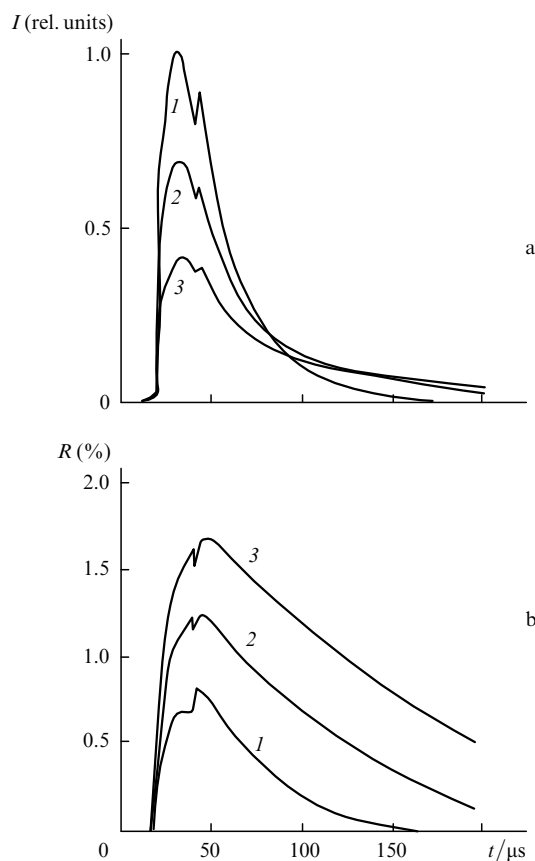


**Figure 7.** Calculated dynamics of the intensity of lasing (a) and of the reflection coefficient (b) on the individual vibrorotational transitions  $P_{8\rightarrow 7}(17)$  (1),  $P_{9\rightarrow 8}(16)$  (2), and  $P_{10\rightarrow 9}(15)$  (3).

result of three cascade-coupled transitions. One may therefore speak of a qualitative agreement between the theory and experiment for multifrequency emission.

## 7. Conclusions

The phase-conjugate reflection was investigated in the present study by the DFWM method in the active medium of a frequency-selective EBS CO laser. The maximum energy efficiency of the phase-conjugate reflection reached 1.5–2.5% for emission as a result of one vibrorotational transition, whereas on expansion of the emission spectrum the efficiency of phase conjugation diminished. The duration of a laser-radiation pulse, its intensity within the cavity, and the specific input energy hardly affect the energy efficiency of the phase-conjugate reflection. The density of the gas mixture and the ratio of the intensities of the probe and copropagating reference waves influence the energy reflection coefficient of a phase-conjugate mirror to a greater extent.

Analysis of the temporal properties of phase conjugation by four-wave mixing in the active medium of an EBS CO laser, operating in the free-running regime, permits the conclusion that, under the conditions of the experiments carried out, the phase conjugation is a quasi-cw process throughout the radiation pulse (100–500  $\mu$ s), whereas the duration of the spiky transient process is 1–2  $\mu$ s.

The experimental efficiency of the phase-conjugate reflection was appreciably less than the values predicted by the theory which describes the interaction of the radiation in

an idealised DFWM configuration in the active medium of a frequency-selective EBS CO laser. A quantitative agreement with experimental data within the framework of the theoretical model is attained with decrease in the effective interaction length, which may be associated with the instability of the structure of the cavity mode. The inhomogeneity of the pump power and the variation of the gas temperature and of the intensities of the interacting waves are manifested in a real experiment and may influence the agreement between the theory and experiment.

Comparison of the experimental and calculated (theoretical) temporal dynamics of the reflection coefficient of the phase-conjugate mirror indicates the dominant role of the resonance amplitude phase-conjugation mechanism on the gain gratings in the active medium of an EBS CO laser. The theoretical model describes qualitatively correctly the dependence of the efficiency of phase conjugation by four-wave mixing in the cavity on the ratio of the intensities of the interacting waves and the decrease in the energy reflection coefficient as the operating regime of a frequency-selective EBS CO laser changes from lasing as a result of one vibro-rotational transition to simultaneous lasing as a result of three cascade-coupled transitions.

## References

- Galushkin M G, Dimakov S A, Onoshko R N, et al. *Izv. Akad. Nauk SSSR Ser. Fiz.* **54** 1042 (1990)
- Ageichik A A, Dimakov C A, Rezunkov Yu A, et al. *Proc. SPIE Int. Soc. Opt. Eng.* **1840** 166 (1991)
- Galushkin M G, Ionin A A, Kotkov A A, et al. *Kvantovaya Elektron. (Moscow)* **25** 739 (1998) [*Quantum Electron.* **28** 719 (1998)]
- Galushkin M G, Ionin A A, Kotkov A A, Mitin K V *Kvantovaya Elektron. (Moscow)* **25** 905 (1998) [*Quantum Electron.* **28** 881 (1998)]
- Belousov D V, Borodin A M, Bunkina M V, et al. *Fourteenth International Conference on Coherent and Nonlinear Optics, Leningrad, 1991, Vol. 1, p. 177*
- Berdyshev A V, Borodin A M, Gurashvili V A, et al. *Kvantovaya Elektron. (Moscow)* **23** 47 (1996) [*Quantum Electron.* **26** 45 (1996)]
- Afanas'ev L A, Ionin A A, Kiselev E A, et al. *Kvantovaya Elektron. (Moscow)* **21** 557 (1994) [*Quantum Electron.* **24** 513 (1994)]
- Berdyshev A V, Kurnosov A K, Napartovich A P *Kvantovaya Elektron. (Moscow)* **20** 529 (1993) [*Quantum Electron.* **23** 455 (1993)]
- Berdyshev A V, Kurnosov A K, Napartovich A P *Kvantovaya Elektron. (Moscow)* **21** 91 (1994) [*Quantum Electron.* **24** 87 (1994)]
- Belykh A D, Gurashvili V A, Kochetov I V, et al. *Kvantovaya Elektron. (Moscow)* **22** 333 (1995) [*Quantum Electron.* **25** 315 (1995)]
- Ionin A A, Klimachev Yu M, Kobsa H, Sinitsin D V *Kvantovaya Elektron. (Moscow)* **24** 195 (1997) [*Quantum Electron.* **27** 189 (1997)]
- Beairsto C, Walter R, Ionin A, et al. *Kvantovaya Elektron. (Moscow)* **24** 631 (1997) [*Quantum Electron.* **27** 614 (1997)]
- Afanas'ev L, Ionin A, Klimachev Yu, et al. *Proc. SPIE Int. Soc. Opt. Eng.* **3092** 142 (1996)]
- Afanas'ev L A, Galushkin M G, Ionin A A, et al. *Izv. Akad. Nauk SSSR Ser. Fiz.* **60** 41 (1996)
- Islamov R Sh, Konev Yu B, Kochetov I V, Kurnosov A K *Kvantovaya Elektron. (Moscow)* **11** 210 (1984) [*Sov. J. Quantum Electron.* **14** 147 (1984)]
- Zel'dovich B Ya, Pilipetsky N F, Shkunov V V *Principles of Phase Conjugation* (Berlin: Springer, 1985)